Scalable Large-Signal Device Model for High Power-Density AlGaN/GaN HEMTs on SiC

Jong-Wook Lee, Sungjae Lee and Kevin J. Webb
School of Electrical and Computer Engineering
Purdue University, West Lafayette, IN 47907-1285

Abstract— **A scalable device model for high-power, large periphery AlGaN/GaN HEMTs on SiC has been developed which includes device self-heating. The parameterized model coefficients were evaluated using S-parameters obtained from isothermal bias contours and pulsed I-V measurements. Model scaling with device size was examined by comparing with measurements for peripheries from 0.25 mm to 1.5 mm. The scaled model showed good agreement with measured S-parameters and power sweep data.**

I. Introduction

Wide bandgap AlGaN/GaN HEMTs on semi-insulating SiC substrates have yielded a power density of 6.9 W/mm at 10 GHz and 9.1 W/mm at 8.2 GHz, making them candidates for compact, light-weight, high power amplifier systems [1], [2]. A compact MMIC power amplifier of 20 Watts at 9 GHz and a hybrid flip-chip amplifier of 14 Watts at 8 GHz were reported using GaN/AlGaN HEMTs on SiC [3], [4]. For design purposes, an accurate device model for large periphery devices is critical to fully utilize high power density devices. A model for a GaN HEMT on sapphire, valid without device heating, has recently been reported [5], and simulated and measured results agreed well when used to simulate a monolithic GaN distributed amplifier [6]. However, inclusion of heating effects would allow a better description of large periphery devices operating with high power dissipation.

We have used a modified Curtice cubic model which includes temperature-dependent device characteristics. Device parameters have been extracted using S-parameter data measured on isothermal contours and pulsed I-V curves. We examined device scalability by measuring devices up to 1.5 mm and estimating the temperature rise due to power dissipation. This resulted in a scalable, temperature-dependent model for a GaN HEMT on SiC. Power sweep measurements for device peripheries up to 1.5 mm support the accuracy of the model.

II. Pulsed I-V Measurement and Temperature Effects

Pulsed I-V measurements allow the extraction of model parameters, permitting accurate determination of transconductance, frequency dispersion, and trapping effects [7]. Pulsed I-V characteristics were measured for a 250 μm AlGaN/GaN HEMT by pulsing the drain voltage, V_{ds}, with pulses of 1 μsec duration and 1 kHz repetition rate at V_{gs}=0, V_{ds}=0. This pulsing and duty cycle allows I-V measurement with negligible DC power dissipation, and

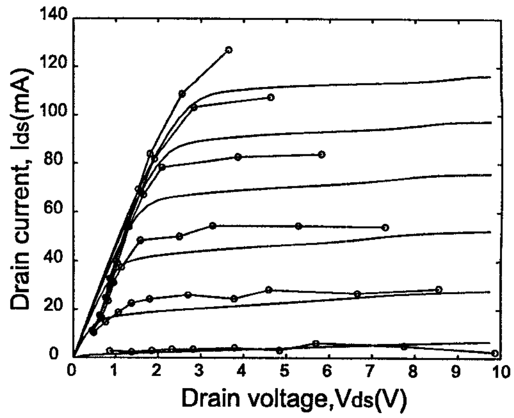

Fig. 1. Pulsed and static I-V characteristic of a 250 μm GaN HEMT on SiC. V_{gs}=-2.5 V to V_{gs}=0 V, with a step of 0.5 V (line: static, symbol: pulsed)

a comparison with the static (CW) I-V curves is shown in Figure 1. The static I-V approaches the pulsed I-V at low drain current, while the two differ significantly at larger drain current.

The influence of heating is observed in the static I-V curves of Figure 2 for the same discrete 1.5 mm device mounted on silicon and copper substrates using epoxy. The current difference becomes large as the power dissipation increases, and more current droop occurred with the device mounted on the silicon substrate.

III. Systemic Determination of Drain Current Modeling Coefficient

Significant device heating can occur with high drain bias, typically 20-40V for GaN HEMTs, and high RF power. Therefore, a temperature-dependent model is necessary. A small, 250 μm periphery, two-finger HEMT was modeled using an Agilent EEsof LIBRA user-defined nonlinear model with a circuit for self-heating. The topology of this model, called CFET2 [8], is given in Figure 3. The current source, I_{th}, is numerically equal to the instantaneous power dissipated in the FET and the resistance, R_{th}, is the thermal resistance. The $R_{th}C_{th}$ product, τ_{th}, is the thermal time constant. Previously, an electro-thermal nonlinear model for a silicon RF LDMOS FET used a temperature-dependent current equation [9].

As the conventional device modeling approach based on fitting static I-V curves is not an accurate indicator of the

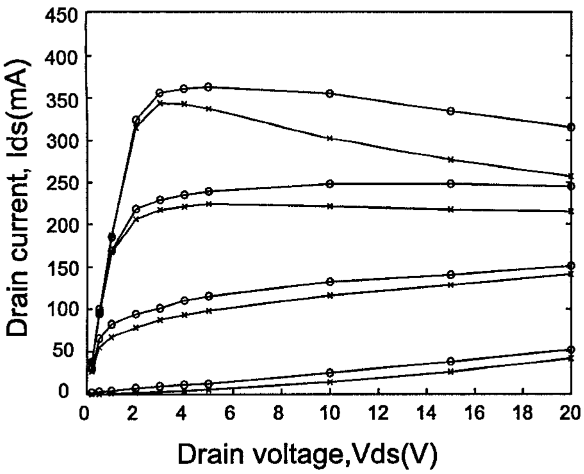

Fig. 2. Measured static drain current characteristic for a 1.5 mm GaN HEMT on two heat sink materials (x-: silicon, o-: copper). V_{gs}=-3.0 V, step 0.5 V.

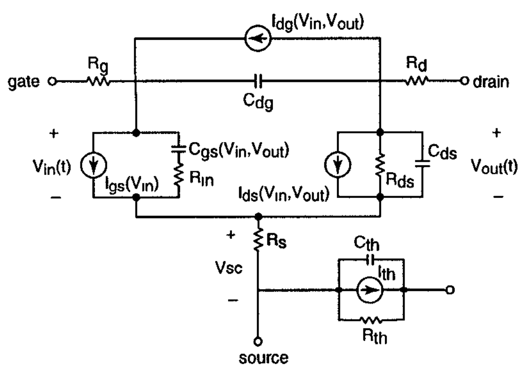

Fig. 3. Large signal model topology including a thermal equivalent circuit.

measured power spectrum, due to RF dispersion and thermal heating [7], a more accurate approach is necessary for high power GaN devices. A bias-dependent large-signal model using pulsed isothermal characterization has been reported [10], but the S-parameter measurement employed with pulsed bias is time consuming without specialized equipment. We propose extraction of the drain current coefficients using isothermal small signal S-parameter measurements with static bias, providing an accurate model with standard equipment.

Consider the Curtice cubic model [8] with temperature-dependent current modeling coefficients $A_i(T)$ and g_m, which can be represented as

$$g_m = (A_1(T) + 2A_2(T)V_1 + 3A_3(T)V_1^2)\tanh(\gamma V_{out}) \times (1 + \lambda V_{out})(1 + \beta(V_{dso} - V_{out})), \quad (1)$$

where $V_1 = V_{in}(t - \tau)(1 + \beta(V_{dso} - V_{out}))$, with V_{dso} the drain voltage where A_i is extracted, and where β describes the pinch-off dependence on V_{ds}, γ is the drain current saturation parameter, λ is the drain current coefficient, V_{out}

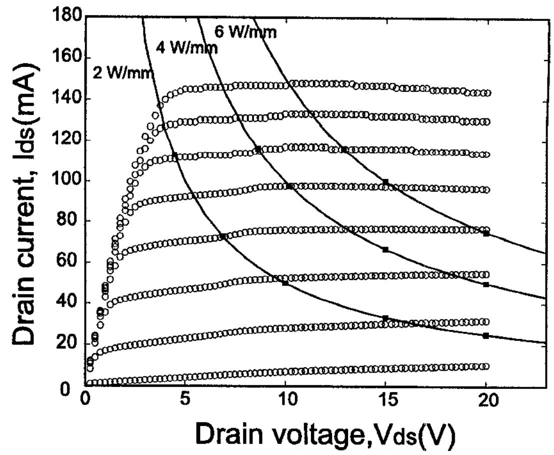

Fig. 4. Measured drain current of 250 μm device and 2 W/mm, 4 W/mm, and 6 W/mm isothermal contours. V_{gs}=-2.5 V to V_{gs}=1.0 V, with a step of 0.5 V. The model uses temperature-dependent coefficients obtained from S-parameters measured on isothermal contour.

is the steady-state harmonic balance solution. The drain current can be represented as

$$I_{ds} = (A_0(T) + A_1(T)V_1 + A_2(T)V_1^2 + A_3(T)V_1^3) \times \tanh(\gamma V_{out})(1 + \lambda V_{out}). \quad (2)$$

The coefficients $A_i(T_0)$ with negligible power dissipation can be evaluated from the pulsed I-V measurement, and $A_i(T)$ can be determined from the static I-V and S-parameters measured along various isothermal bias contours. From (1) and (2), we note that the static value of $A_0(T)$ can be determined from the static drain current at V_1=0, but the operating value of $A_0(T)$ is determined using S-parameters on isothermal contours. $A_1(T)$ is known from the g_m at V_{gs}=0, measured on an isothermal contour. Therefore,

$$A_0(T) = \frac{1}{\alpha_1} I_{ds}|_{V_1=0}, \quad A_1(T) = \frac{1}{\alpha_2} g_m|_{V_1=0}, \quad (3)$$

where $\alpha_1 = \tanh(\gamma V_{out})(1 + \lambda V_{out})$ and $\alpha_2 = \tanh(\gamma V_{out})(1 + \lambda V_{out})(1 + \beta(V_{dso} - V_{out}))$ in the saturation region. Using two or more different measurements at isothermal bias points, the remaining $A_i(T)$ can be determined. Figure 4 shows measured static I-V curves along with three isothermal contours.

Drain current coefficients evaluated using static I-V, pulsed I-V, and isothermal S-parameters are given in Table I. The temperature rise T_0, T_1, and T_2 correspond to negligible heating, 2 W/mm, and 4 W/mm, respectively. To investigate the extent of heating in the devices and extract the thermal model parameters in Figure 3, the channel temperature and thermal resistance is needed. Using the device geometry and measured DC characteristics, channel temperature rise was obtained as a function of drain bias for Class A and Class AB(B) operation. An analytic FET thermal resistance model [11] was used under the assumption

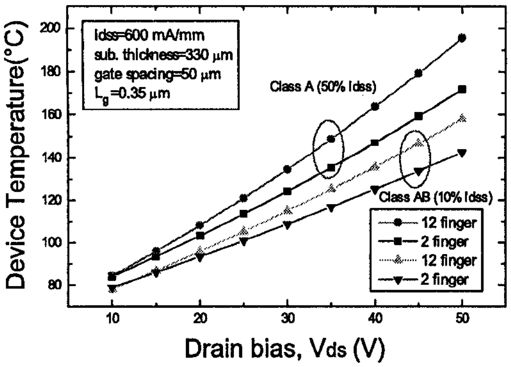

Fig. 5. Temperature rise versus drain bias voltage for 2 finger (250 μm) and 12 finger (1.5 mm) GaN HEMTs on SiC under Class A and Class AB mode operation

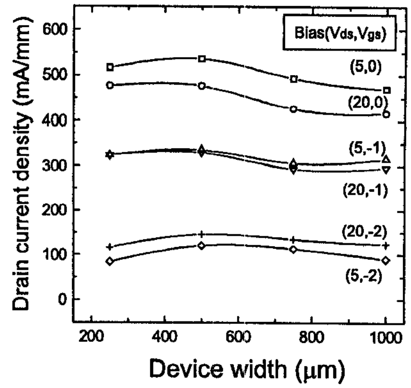

Fig. 6. Drain current density as a function of the device width for GaN HEMT on SiC

that the gate segments are the heat source, and maximum power is produced for each drain bias. The temperature for an example GaN HEMT is shown in Figure 5 for Class A and Class AB bias, as a function of drain voltage, with the specified drain current and device geometry.

From the simulated temperature, a thermal resistance was calculated. This resulted in R_{th}=33.81 K/W for the 0.25 mm device, 8.45 K/W for the 1.0 mm device, and 6.38 K/W for the 1.5 mm device. With the drain current and thermal model coefficients determined, the remaining extrinsic and intrinsic parameters extracted from isothermal S-parameters were used as input parameters to the CFET2 large signal model. The set of parameters thus determined is given in Table II.

TABLE I

Temperature-dependent drain current modeling coefficients for 0.25 *mm* periphery GaN HEMT.

$\times 10^{-3}$	CW	$A_i(T_0)$	$A_i(T_1)$	$A_i(T_2)$
A_0	116.1	142.1	132.3	114.8
A_1	35.97	54.97	-13.9	37.3
A_2	-4.874	-2.121	-43.5	-13.3
A_3	-0.8052	-0.7567	-8.60	-3.02

TABLE II

Modified Curtice cubic model parameters for 0.25 *mm* periphery GaN HEMT.

Resistance	Capacitance	Thermal	Diode
R_g=3.305Ω	C_{gs}=0.268pF	R_{th}=33.81	V_{BI}=2.35V
R_d=2.534Ω	C_{gd}=10.93fF	$\tau_{th} = 10^{-6}$ s	I_s=0.27μA
R_s=0.382Ω	C_{ds}=15.87fF	T_{tmph}=85°C	R_1=1000Ω
R_{in}=2.58Ω		T_{tsnk}=27°C	R_2=45Ω
R_{ds}=736Ω		T_{tmp}=27°C	

IV. Scalability of GaN HEMTs and Model Verification

Device model scaling was examined on two device geometries. One is a 2-finger device, and the device size increases with finger length (0.5 mm, 0.75 mm and 1.0 mm), where the thermal dissipation density is similar. The other is a 1.5 mm device (12 × 125 μm) with sources connected by air bridges, and higher thermal dissipation is expected. With the extracted large signal model for a 250 μm device, the scaled models for 0.5 mm and 1.0 mm devices were constructed with a distributed gate model, where the elementary cell is connected in series. The device model of the 1.5 mm device was constructed by area scaling a two-finger 250 μm model and then fitting the model to measured S-parameters. Scalability of the drain current, S-parameters, and CW power sweep were examined. The measured CW drain current of the 2-finger devices scaled well, as shown in Figure 6, although heating resulted in decreased current at the higher drain biases. Figure 7 shows the good agreement between measured and modeled S-parameters for 0.25 mm, 0.5 mm and 1 mm devices. Figure 8 shows the comparison of modeled and measured power output and PAE of the 0.25 mm, 0.5 mm and 1.0 mm devices. The power was measured in a 50 Ω system, which is suitable for modeling verification purposes, and the PAE improved for larger devices because the load better matches the 50 Ω system. Figure 9 shows the measured and modeled output power, PAE, drain DC current, and gain of the 1.5 mm device, with good agreement.

V. Conclusion

A simple and accurate modeling approach, based on a modified Curtice model, has been developed for high power density AlGaN/GaN HEMTs. Temperature-dependent drain current coefficients were extracted from measured isothermal S-parameters and pulsed I-V data. Devices of size 0.25 mm to 1.5 mm were measured and accurately modeled using this approach.

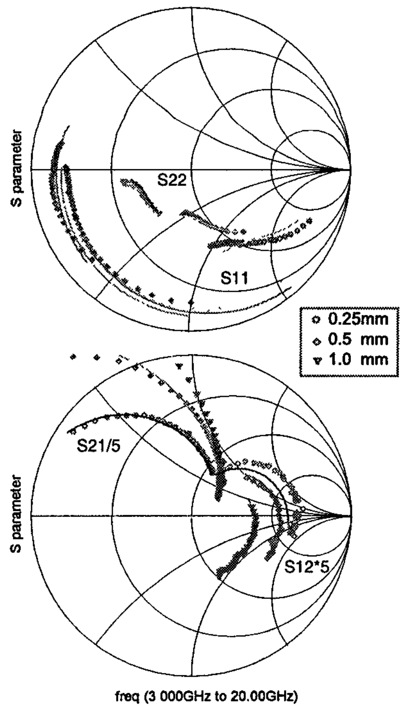

Fig. 7. Measured and modeled S-parameters for 0.25 mm, 0.5 mm and 1 mm GaN HEMTs at V_{ds}=15 V, V_{gs}=-2.2 V(symbols: measurement, lines: simulation.)

VI. Acknowledgments

The authors would like to thank W. R. Curtice, S. T. Sheppard, and L. F. Eastman for their input on this work. Funding came from ONR (# N00014-98-1-0371 and N0014-99-C-0172, monitored by John Zolper). The devices were fabricated by Cree, Inc. under contracts from ONR (# N00014-99-C-0172, John Zolper) and AFRL (# F33615-99-2-1472, Tom Jenkins).

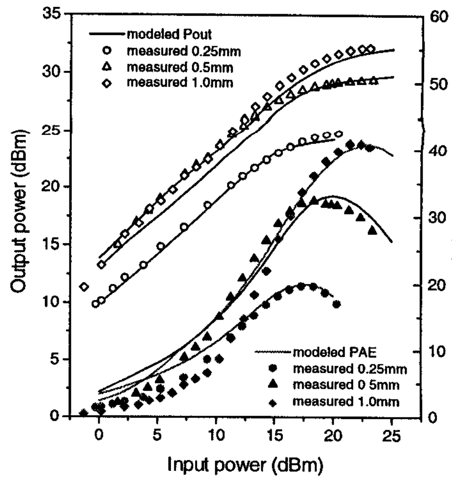

Fig. 8. A 4 GHz CW power sweep for 0.25 mm, 0.5 mm and 1 mm GaN HEMTs on 4H-SiC at V_{ds}=15V, V_{gs}=-2.2V

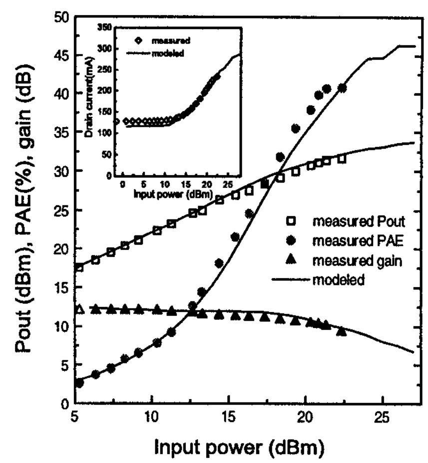

Fig. 9. A 4 GHz CW power sweep of 1.5 mm GaN HEMT on 4H-SiC at V_{ds}=15 V, V_{gs}=-2.6V.

References

[1] S. T. Sheppard, K. Doverspike, W. L. Pribble, S. T. Allen, J. W. Palmour, L. T. Kehias, and T. J. Jenkins, "High-power microwave GaN/AlGaN HEMTs on semi-insulating silicon carbide substrates," *IEEE Electron Device Lett.*, vol. 20, no. 4, pp. 161–163, Apr. 1999.

[2] Y.-F. Wu, D. Kapolnek, J. Ibbetson, N.-Q.Zhang, P. Parikh, B. P. Keller, and U. K. Mishra, "High Al-content AlGaN/GaN HEMTs on SiC substrates with very high power performance," in *IEDM Technical Digest*, Dec. 1999, pp. 925–927.

[3] S. T. Sheppard, W. L Pribble, D. T. Emerson, Z. Ring, R. P. Smith, S. T. Allen, J. W. Milligan, and J. W. Palmour, "Technology development for GaN/AlGaN HEMT MMIC amplifiers on semi-insulating SiC substrates," in *IEEE/Cornell University Conference on Advanced Concepts in High Performance Devices*, Aug. 2000.

[4] Y.-F. Wu, D. Kapolnek, J. Ibbetson, P. Parikh, B. P. Keller, and U. K. Mishra, "14-W GaN-based microwave power amplifier," in *IEEE MTT-S Int. Microwave Symp. Dig.*, 2000, vol. 2, pp. 963–965.

[5] B. M. Green, H. Kim, K. K. Chu, H. S. Lin, V. Tilak, J. R. Shealy, J. A. Smart, and L. F. Eastman, "Validation of an analytic large signal model for AlGaN/GaN HEMTs," in *IEEE MTT-S Int. Microwave Symp. Dig.*, 2000, vol. 2, pp. 761–764.

[6] B. M. Green, S. Lee, K. Chu, K. J. Webb, and L. F. Eastman, "High efficiency monolithic gallium nitride distributed amplifier," *IEEE Microwave Guided Wave Lett.*, vol. 10, no. 7, pp. 270–272, July 2000.

[7] A. Platzker, A. Palevsky, S. Nash, W. Struble, and Y. Tajima, "Characterization of GaAs devices by a versatile pulsed I-V measurement system," in *IEEE MTT-S Int. Microwave Symp. Dig.*, 1990, pp. 1137–1140.

[8] W. R. Curtice Consulting, *CFET User's Manual.*

[9] W. R. Curtice, J. A. Pla, D. Bridges, T. Liang, and E. E. Shumate, "A new dynamic electro-thermal nonlinear model for silicon RF LDMOS FETs," in *IEEE MTT-S Int. Microwave Symp. Dig.*, 1999, vol. 2, pp. 419–423.

[10] J-P. Teyssier, P. Bouysse, Z. Ouarch, D. Barataud, T. Peyretaillade, and R. Quere, "40-GHz/150-ns versatile pulsed measurement system for microwave transistor isothermal characterization," *IEEE Trans. Microwave Theory Tech.*, vol. 46, no. 12, pp. 2043–2052, Dec. 1998.

[11] H. F. Cooke, "Precise technique finds FET thermal resistance," *Microwave & RF*, vol. 25, pp. 85–87, Aug. 1981.